International Journal of the Physical Sciences Vol. 6(3), pp. 540-549, 4 February, 2011
Available online at http://www.academicjournals.org/IJPS
DOI: 10.5897/IJPS10.586
ISSN 1992 - 1950 ©2011 Academic Journals

Full Length Research Paper

Pan evaporation analysis in central México: Trends, self-affinity and important frequencies

Fidel Blanco-Macías[1], Ricardo D. Valdez-Cepeda[1,2] and Rafael Magallanes-Quintanar[3]*

[1]Universidad Autónoma Chapingo, Centro Regional Universitario Centro–Norte. Calle Cruz del Sur No. 100, Col. Constelación. Apdo. Postal 196, CP 98085, El Orito, Zacatecas, Zac., México.
[2]Universidad Autónoma de Zacatecas, Unidad Académica de Matemáticas. Calzada Solidaridad s/n. CP 98064, Zacatecas, Zac., México.
[3]Universidad Autónoma de Zacatecas, Unidad Académica de Ingeniería Eléctrica. Ave. Ramón López Velarde 801, CP 98064, Zacatecas, Zac., México.

Accepted 13 January, 2011

Long-term monthly pan evaporation time series registered at 40 meteorological stations located within Mexico's state of Zacatecas were analyzed in order to identify their trends. In addition, we analyzed the power spectrum signals of evaporation anomaly series in order to identify their important frequencies and its possible connection with periodic phenomena. Results suggest that negative trends are prevailing over positive trends. We found negative linear trend for 27 out of 40 pan evaporation time series; 18 of the 27 decreasing trends were significant at $p<0.05$. On the other hand, 13 out of 40 pan evaporation trends were positive but only 3 at significant level ($p<0.05$). Moreover, noise in all of these monthly pan evaporation series tends to be a persistent behavior. Additionally, we found that important frequencies could be related with the yearly cycle, quasi–biannual cycle, 'El Niño Southern Oscillation' phenomena and sunspot cycle.

Key words: Linear trends, fractal dimension, power spectrum density, yearly cycle, quasi–biannual cycle, El Niño Southern Oscillation, sunspot cycle.

INTRODUCTION

Historically, most of the studies rely in the traditional view that pan evaporation trends are assumed to mirror trends in terrestrial surface evaporation. The evaporation of water as measured from pan evaporimeters has decreased in many regions of the world over the past half-century (Roderick and Farquhar, 2004), which suggests a recent decrease in the terrestrial evaporation component of the hydrologic cycle (Lawrimore and Peterson, 2000). In the northern hemisphere, widespread decreases in pan evaporation rates, averaging 2 to 4 mm per year, have occurred over several decades up to about 1990 (Gifford et al., 2005). Despite those impressive facts, there is lack of studies about evaporation behavior and its possible relation with periodic phenomena in Mexico, although there is a national network of meteorological stations.

It has generally been expected that evaporation will increase in the future because of increasing temperatures from global warming and an intensifying hydrologic cycle (Huntington, 2006). However, several reports show that land evaporation trend is decreasing (Chattopadhyay and Hulme, 1997; Quintana-Gomez, 1998; Linacre, 2004). To know the behavior of local pan evaporation could be of great socioeconomic importance because in rural areas it is commonly coupled with crop coefficient values for irrigation scheduling and water management (Mutziger et al., 2005). This is the case of arid and semiarid irrigated land areas (150,000 ha) of the Mexican state of Zacatecas, where aquifers are over-exploited with a

*Corresponding author. E-mail: tiquis@gmail.com. Tel: +52 492 9239407 ext. 1215.

deficit of about 201,100,000 m^3 per year (Semarnat, 2008). In addition to the traditional statistical analysis, evaporation time series could be analyzed using other approaches; for instance, they could be treated like fractal profiles. Hence, the aims of this study were: 1) To identify trends of 40 long-term time series of evaporation registered at meteorological stations located within Mexico's state of Zacatecas, and 2) To identify important frequencies and its possible connection with periodic phenomena for 40 long-term evaporation anomaly time series by means of the power spectrum analysis.

MATERIALS AND METHODS

Data

The original data were long-term records of monthly evaporation. We acquired those data sets for 40 meteorological stations located within the territory of the Mexico's state of Zacatecas. Generalities for each station and series are appreciated in Table 1. Data were kindly provided by the 'Comisión Nacional del Agua', the National Official Institution in charge of the registration of climatic and meteorological data in Mexico. Original data sets were treated as fractal profiles to estimate firstly their linear trends by means of regression analysis and later to compute self-affinity indexes of the evaporation anomaly time series by means of fractal analysis through power spectrum approach.

Evaporation linear trends and anomaly series

Climate time series are in general non-stationary, and frequently present long-term trends. Thus removing the trends is an important issue in order to avoid that non-stationary behavior accompanying these data will give spurious results (Peng et al., 1994; Hausdorff and Peng, 1996). When this step is performed, the new time series is known as anomaly time series, which is the time series of deviations of a quantity from some mean (Wilks, 1995). The linear trends were estimated through least squares linear regression analyses taking into account the following simple model:

$$Y_i = a + bX_i \quad (1)$$

Before to carry out the fractal analysis through power spectrum density approach, linear trends of the series were removed following equation 1:

$$Y_{di} = Y_i - (a + bX_i), \quad (2)$$

Where Y_{di} is i_{th} detrended monthly mean evaporation.

Fractal analysis

Temporal variation of natural phenomena has been difficult to characterize and quantify. To solve these problems, fractal analysis was introduced by Mandelbrot (1982). Time series can be characterized by a non-integer dimension (fractal dimension) when treated as random walks or self-affine profiles. Self-affine systems are often characterized by roughness, which is defined as the fluctuation of the height over a length scale. For self-affine profiles, the roughness scales with the linear size of the surface by an exponent called the roughness or Hurst exponent. However, this exponent gives limited information about the underlying distribution of height differences (Evertsz and Berkner, 1995).

There is the fact that the Hurst exponent as well as the fractal dimension measures how far a fractal curve is from any smooth function which one uses to approximate it (Moreira et al., 1994). There are a lot of approaches to estimate fractal dimension for self-affine profiles but we used only the power spectrum technique, because it is sensitive and good exploratory tool for real data (Weber and Talkner, 2001).

Power spectrum approach

Self-affine fractals are generally treated quantitatively using spectral techniques. The variation of the power spectrum P(f) with frequency f appears to follow a power law (Turcotte, 1992):

$$P(f) \sim f^{-\beta}. \quad (3)$$

The power spectrum P(f) is defined as the square of the magnitude of the Fourier transform of the monthly evaporation. Denoting evaporation as a function of time by Z(t), we have:

$$P(f) = \left| \int_{t_0}^{t_1} Z(t) e^{-i2\pi ft}\, dt \right|^2, \quad (4)$$

Where t_0 and t_1 are the limits of time over which the series extend. In the case of such evaporation record, which is sampled at discrete time intervals, we should use the discrete version of Equation 4:

$$P(f) = \left| \sum_{t=t_0}^{t_1} Z(t) e^{-i2\pi ft} \right|^2. \quad (5)$$

The next step is to obtain a relationship between the power β and the fractal dimension D. By considering two time series $Z_1(t)$ and $Z_2(t)$ related by:

$$Z_2(t) = \frac{1}{r^H} Z_1(rt); \quad (6)$$

It can be observed that $Z_1(t)$ has the same statistical properties as $Z_2(t)$, and since Z_2 is a properly rescaled version of Z_1, their power spectral densities must also be properly scaled. Thus we can write:

$$P(f) = \frac{1}{r^{2H+1}} P\left(\frac{f}{r}\right). \quad (7)$$

It follows that,

$$\beta = 2H + 1 = 5 - 2D_s, \quad (8)$$

$$D_s = \frac{5-\beta}{2}, \quad (9)$$

and

$$H = 2 - D_s, \quad (10)$$

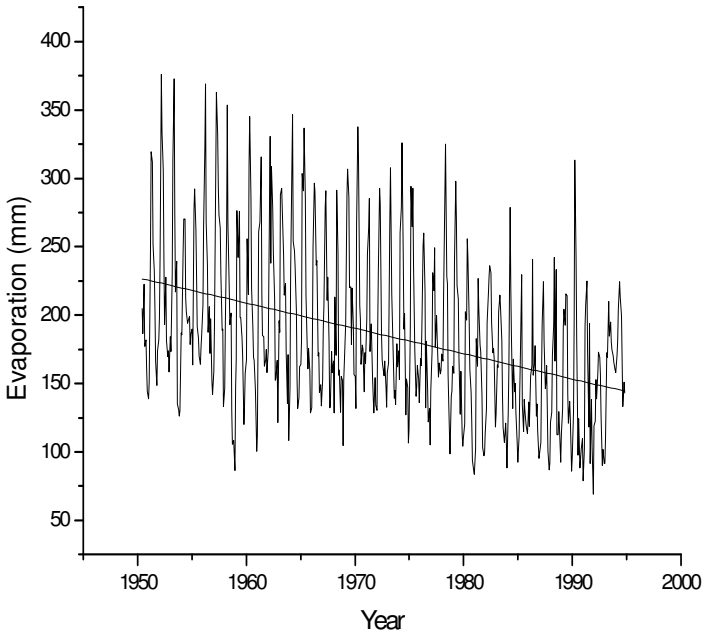

Figure 1. Time series plot of monthly evaporation registered at Trancoso, Zac., México from June, 1950 to November, 1994. The fitted line Y = 3849.05 -1.85X was used to estimate the yearly tendency of -1.85 mm year^{-1}.

Where D_s denotes the fractal dimension estimated from the power spectrum and H is the Hurst exponent. Since the periodogram is a poor estimate of the power spectrum because the estimate of the power at any frequency is very noisy, with the amplitude of the noise being proportional to the spectral power, we preferred to use the artifact of averaging periodograms to obtain 50 regular logarithmic intervals of the two records (complete and partial series). Moreover, we used the 'running sum' transformation to shift, by a factor of +2, the slope, and thereby the Hurst exponent and the D_s because data trace had a slope between -1 and 1 on the log-log plot.

In practice, to obtain an estimate of the fractal dimension D_s, one calculates the power spectrum P(*f*) (where $f = {}^{2p}/_{l}$ *f* is the wave–number, and *l* is the wavelength), and plots the logarithm of P(*f*) versus the logarithms of *f*. If the profile is self-affine, this plot should follow a straight line with a negative slope -β (Valdez–Cepeda et al., 2003a, b). Important frequencies of evaporation anomaly series were estimated using the plot yielded by power-spectral density, $\Phi_x(f)$ vs. frequency by taking into account significant ($p<0.05$) peaks.

RESULTS

Linear trends

As stated previously, pan evaporation has been decreasing in several places around the globe during the last 50 years (Brutsaert 2006; Roderick and Farquhar 2002; Lawrimore and Peterson 2000). In this century, many studies have shown local trends of decreasing pan evaporation. Johnson and Sharma (2010) summarized some overall negative annual pan evaporation trends: Australia (-2 mm year^{-1}), New Zealand (-2.1 mm year^{-1}), China (-2.9 mm year^{-1}), former USSR (-4 mm year^{-1}); United States of America case was found to range from approximately -1.5 to -2 mm yr^{-1}. Also, Gifford et al. (2005) consigned a range from -2 to -4 mm yr^{-1} for the northern hemisphere. In the present study a simple linear regression procedure was performed to 40 pan evaporation time series with the aim to obtain their linear models (Figure 1). Station's generalities and trend analyses results are shown in Table 1.

Negative linear trends were obtained for 27 out of 40 pan evaporation time series; 18 of the 27 decreasing trends were significant at $p<0.05$. On the other hand, 13 pan evaporation trends were positive but only 3 at significant level ($p<0.05$). The overall mean of trends was -0.32 mm year^{-1}; whereas the mean of all significant trends was -0.53 mm year^{-1}. In addition, the mean of significant increasing evaporation trends was 1.09 mm year^{-1}, and the mean of significant decreasing evaporation trends was -0.79 mm year^{-1}.

Power spectrum analysis

Fractality statistics of evaporation time series are given in Table 2. Anomaly time series for all stations with significant trends (23 out of 40) were analyzed and

Table 1. Generalities of meteorological stations and linear trend analysis.

Station name	Coordinates	masl	Period	Months	Y = a + bx	
					a	b
Cedros	24° 40' 43'' N 101° 46' 26'' W	1763	Jan 1979 - Nov 2005	431	-2524.44	**1.35** (p=5.03E-10)
Chalchihuites	23° 14' 27'' N 102° 34' 31'' W	2060	Nov 1966 - Dec 2005	470	-1763.17	0.97 (p=0.142269)
Col. González Ortega	23° 57' 22'' N 103° 27' 02'' W	2190	Jan 1970 - Oct 2003	406	-1113.10	0.65 (p=0.01446)
El Cazadero	23° 41' 35'' N 103° 26' 50'	1898	Jun 1959 - Dec 2005	564	-244.20	0.21 (p=0.22826)
El Platanito	22° 36' 43'' N 104° 03' 05'' W	990	Jul 1957 - Dec 2005	582	1290.05	**0.75** (p=2.20E-4)
El Rusio	22° 26' 34'' N 101° 47' 09'' W	2104	Jan 1967 - Dec 2005	468	1400.71	**-0.61** (p=0.00362)
El Sauz	23° 10' 46'' N 103° 01' 26'' W	2090	Jan 1947 - Dec 2005	707	1139.34	**-0.49** (p=0.546E-5)
Excame III	21° 38' 58'' N 103° 20' 23'' W	1740	Jan 1946 - Nov 2005	719	2656.99	**-1.26** (p=0)
Fresnillo	23° 10' 22'' N 102° 56' 26'' W	2195	Sep 1949 - Dec 2005	676	1348.22	**-0.59** (p=4.47E-5)
Gral. Guadalupe Victoria	22° 23' 43'' N 101° 49' 52'' W	2183	Jan 1966 - Dec 2005	480	1529.21	**-0.69** (p=8.40E-5)
Gruñidora	24° 16' 19'' N 101° 53' 05'' W	1825	Jan 1963 - Dec 2005	516	-2164.86	**1.17** (p=2.77E-8)
Huanusco	21° 46' 01'' N 102° 58' 07'' W	1495	Jan 1972 - Feb 2005	398	1748.48	**-0.79** (p=0.00518)

Table 1. Contd.

Jerez	22° 38' 31'' N 103° 00' 05'' W	2098	Aug 1962 - Dec 2005	521	3909.85	**-1.88** (p<0)
Jiménez del Téul	23° 15' 18'' N 103° 47' 54'' W	1900	Aug 1962 - Dec 2005	520	1298.81	**-0.57** (p<5.09E-4)
Juchipila	21° 23' 14'' N 103° 06' 53'' W	1270	Jan 1947 - Dec 2005	708	807.32	**-0.31** (p<0.00765)
La Florida	22° 41' 10'' N 103° 36' 09'' W	1870	Jul 1954 - Nov 2005	617	89.56	**0.03** (p<0.84511)
La Villita	21° 36' 08'' N 103° 20' 13'' W	1790	Jul 1957 - Dec 2005	582	1460.08	**-0.65** (p<5.14E-4)
Loreto	22° 16' 50'' N 101° 56' 50'' W	2029	Jan 1963 - Dec 2005	516	252.36	**0.21** (p<0.25449)
Monte Escobedo	22° 19' 32'' N 103° 29' 38'' W	2190	Sep 1963 - Dec 2005	508	1489.13	**-0.67** (p<8.40E-4)
Nochistlán de Mejía	21° 21' 55'' N 103° 50' 32'' W	1850	Oct 1949 - Jun 2001	621	114.57	0.03 (p<0.83059)
Ojocaliente	22° 24' 38'' N 102° 16' 09'' W	2050	Aug 1959 - May 2006	562	57.33	0.05 (p<0.71859)
Palomas	22° 20' 47'' N 102° 47' 48'' W	2030	Mar 1969 - Dec 2005	442	423.63	-0.11 (p<0.70594)
Pinos	22° 16' 54'' N 101° 34' 47'' W	2408	Jan 1947 - Mar 2006	711	41.74	0.06 (p<0.54835)
Presa El Chique	22° 00' 00'' N 102° 53' 23'' W	1620	Jan 1963 - Dec 2005	516	2066.01	**-0.95** (p<3.78E-5)
San Antonio del Ciprés	22° 56' 08'' N 102° 29' 14'' W	2145	Jan 1969 - Nov 2005	443	53.62	**0.07** (p<0.76251)

Table 1. Contd.

San Gil	24° 11' 43'' N 102° 58' 36'' W	1810	Aug 1969 - Apr 2006	441	1594.58	**-0.71** (p<0.00502)
San Isidro de los González	22° 50' 41'' N 103° 22' 57'' W	2000	Jan 1976 - May 2006	360	710.52	**-0.27** (p<0.43297)
San Pedro Piedra Gorda	22° 27' 09'' N 102° 20' 49'' W	2032	Jan 1943 - Jun 2006	762	1302.66	**-0.57** (p<6.62E-8)
Santa Lucía	22° 26' 03'' N 104° 13' 00'' W	2252	Aug 1972 - Oct 2004	387	779.50	**-0.31** (p<0.29352)
Santa Rosa	22° 55' 34'' N 103° 06' 47'' W	2240	Jan 1947 - Dec 2005	708	1024.98	**-0.43** (p<6.01E-4)
Tayahua	22° 07' 13'' N 102° 51' 46'' W	1549	Jan 1973 - Dec 2005	396	1473.74	**-0.65** (p<0.01347)
Tecomate	21° 32' 40'' N 103° 02' 32'' W	1375	Jan 1947 - Jul 1997	607	2740.37	**-1.29** (p<7.64E-13)
Teúl de González Ortega	21° 27' 42'' N 103° 27' 52'' W	1900	Oct 1962 - Dec 2005	619	1801.34	**-0.83** (p<1.91E-6)
Tlaltenango	21° 46' 54'' N 103° 17' 45'' W	1700	Jul 1949 - Dec 2005	678	2119.65	**–0.98** (p<1.03E-14)
Trancoso	22° 44' 39'' N 102° 22' 10'' W	2190	Jun 1950 - Nov 1994	534	3839.05	**-1.85** (p<0)
Villa de Cos	23° 17' 26'' N 102° 20' 44'' W	2050	Jan 1962 - Dec 2005	528	370.47	**-0.10** (p<0.59771)
Villa García	22° 10' 10'' N 101° 57' 27'' W	2120	Jan 1959 - Oct 2004	550	1130.35	**-0.49** (p<0.00251)
Villa Hidalgo	22° 20' 49'' N 101° 42' 55'' W	2167	Jan 1954 - Apr 2006	628	668.92	-0.25 (p<0.07253)

Table 1. Contd.

Villanueva	22° 21' 43'' N 102° 53' 22'' W	1920	Jan 1963 - Dec 2005	516	-144.55	0.16 (p<0.40962)
Zacatecas	22° 45' 39'' N 102° 34' 30'W	2485	Jun 1963 - Dec 2003	633	396.91	-0.11 (p<0.45179)

Significant linear trends at p<0.05 are in bold.

Table 2. Self-affinity statistics (Fractal dimension, Ds; Hurst exponent, H; and slope, -β) and identified frequencies (years) for evaporation anomaly time series with linear significant tendencies.

Station name	Coordinates	Self–affinity parameters			Periods (years) of the important identified important frequencies													
		Ds	H	-β	1	2	3	4	5	6	7	8	9	10	11	12	13	14
Cedros	24° 40' 43'' N 101° 46' 26'' W	1.32	0.68	2.36	1.0	2.0	3.7	4.0										
El Platanito	22° 36' 43'' N 104° 03' 05'' W	1.32	0.68	2.36	1.0	2.0	3.0	4.0			7.0							
El Rusio	22° 26' 34'' N 101° 47' 09'' W	1.27	0.73	2.46	1.0		3.0	4.0		6.0					11.0			
El Sauz	23° 10' 46'' N 103° 01' 26'' W	1.27	0.73	2.45	1.0				5.0	6.0	7.0			10.0			13.0	
Excame III	21° 38' 58'' N 103° 20' 23'' W	1.20	0.81	2.61	1.0	2.0	3.0			6.0		8.0			11.0			
Fresnillo	23° 10' 22'' N 102° 56' 26'' W	1.48	0.52	2.04	1.0	2.0		4.0		6.0	7.0		9.0					14.0
Gral. Victoria Guadalupe	22° 23' 43'' N 101° 49' 52'' W	1.30	0.70	2.40	1.0	2.0	3.0	4.0		6.0		8.0					13.0	
Gruñidora	24° 16' 19'' N 101° 53' 05'' W	1.15	0.85	2.70	1.0	2.0	3.0	4.0	5.0		7.0				11.0			
Huanusco	21° 46' 01'' N 102° 58' 07'' W	1.31	0.70	2.39	1.0	2.0		4.0		6.0					11.0			

Table 2. Contd.

Huanusco	21° 46' 01" N 102° 58' 07" W	1.31	0.70	2.39	1.0	2.0		4.0		6.0				11.0			
Jerez	22° 38' 31" N 103° 00' 05" W	1.09	0.91	2.83	1.0		3.0	4.0	5.0		7.0			10.0			14.0
Jiménez del Téul	23° 15' 18" N 103° 47' 54" W	1.25	0.75	2.50	1.0	2.0	3.0	4.0		6.0				11.0			
Juchipila	21° 23' 14" N 103° 06' 53" W	1.28	0.72	2.44	1.00	2.7	3.7	4.2	5.0					10.3			
La Villita	21° 36' 08" N 103° 20' 13" W	1.42	0.59	2.17	1.0	2.6	3.0		5.6		7.0	8.7					
Monte Escobedo	22° 19' 32" N 103° 29' 38" W	1.26	0.74	2.48	1.0		3.0	4.7	5.8		7.0						14.0
Presa El Chique	22° 00' 00" N 102° 53' 23" W	1.17	0.83	2.66	1.0	2.0		4.0			7.0		9.7				
San Gil	24° 11' 43" N 102° 58' 36" W	1.27	0.73	2.47	1.0	2.0	3.0	4.0	5.0								
San Pedro Piedra Gorda	22° 27' 09" N 102° 20' 49" W	1.21	0.79	2.58	1.0	2.0		4.0				8.0			12.0		
Santa Rosa	22° 55' 34" N 103° 06' 47" W	1.39	0.61	2.22	1.0	2.0	3.3	4.0			7.0	8.0					
El Tecomate	21° 32' 40" N 103° 02' 32" W	1.21	0.79	2.58	1.0	2.0	3.0				7.0						
Teúl de González Ortega	21° 27' 42" N 103° 27' 52" W	1.27	0.74	2.47	1.0	2.0	3.5	4.0	5.5	6.30	7.8						
Tlaltenango	21° 46' 54" N 103° 17' 45" W	1.27	0.73	2.45	1.0	2.0	3.0	4.7			7.0	8.3	9.7				
Trancoso	22° 44' 39" N 102° 22' 10" W	1.33	0.67	2.33	1.0		3.0	4.0					9.0				
Villa García	22° 10' 10" N 101° 57' 27" W	1.28	0.72	2.44	1.0	2.8		4.2	5.3		7.0		9.5				

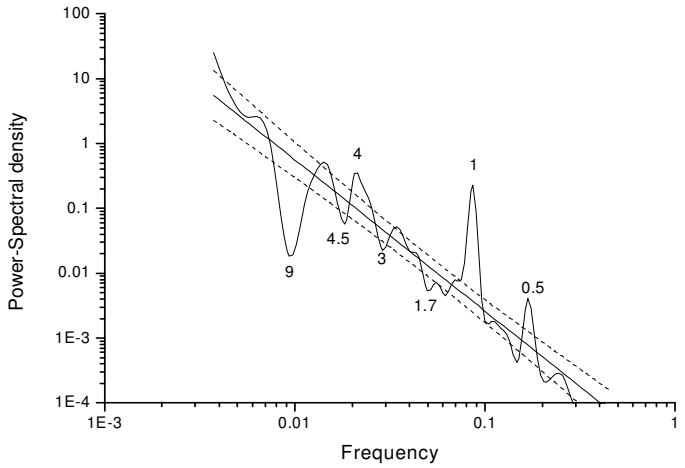

Figure 2. Power spectrum plot of the monthly evaporation anomaly series for Trancoso, Zac., México from June, 1950 to November, 1994. The power-spectral density is given as a function of frequency for time scales of 2 to 534 months. The fitted line was used to estimate the fractal dimension (D_s). $Y = -4.918\ X^{-2.33}$, adjusted r^2 = 0.8759. $D_s = [(5 - \beta)/2]$; $D_s = [(5 - 2.333)/2]$; $D_s = 1.334$.

yielded straight lines on the log–log plot with slope (-β) varying from -2.36 to -2.83 suggesting that $P(f) \propto f^{-\beta}$. Therefore, it means the spectrum is singular and is represented by a curve on the complex plane in all the 23 cases. D_s values vary from 1.32 to 1.48, and H values vary from 0.52 to 0.68. Thus, noise in these monthly evaporation series tends to be persistent (long-term memory) behavior (de la Fuente et al., 1999). As a result, we find that long-term variation is more important than short–term variation in all analyzed profiles of evaporation.

Important frequencies

Plots of power spectrum density, $\Phi_x(f)$ versus frequency allows us to identify the dominant frequencies on evaporation anomaly series, as in terms of the dominant frequencies (1/year) that are likely to be important to the evaporation process. Table 2 show results only for 23 series with significant linear trends. Readers must take note that this approach give us some components of frequency that do not take into account time and length because this analysis give us a resolution in frequency that is determined for the window size over the analyzed time series. In other words, the results shown in Figure 2 give us useful information about the frequency contents of the analyzed series, but they do not indicate at which time these frequencies occurs.

In all analyzed evaporation anomaly time series, annual frequency was present in its power-spectrum. This result is evident because evaporation process is strongly influenced by earth movement around the sun that causes seasons. In 18 out of 23 stations the quasi-biannual cycle was present. Quasi-biannual cycle is a 26 month cycle explaining the reversal in the wind in the lower stratosphere of North pole and solar activity (Labitske and van, 1989; Mendoza et al., 2001). The possible effect of a periodic event like 'El Niño Southern Oscillation' (ENSO) with an erratic cycle from 3 to 5 years (Weber and Talkner, 2001), 3 to 6 years (Monetti et al., 2003) or 2 to 7 years (Zubair, 2002; MacMynowski and Tziperman, 2008) was present in 11 series. The possible effect of sunspots cycle that varies from 8 to 14 years (Mendoza et al., 2001) with a long-term average of 11.3 years was present in 8 stations.

It is noted that 14 periodicities from 8 to 14 years were identified in the longer series as can be appreciated in Tables 1 and 2.

DISCUSSION

Prior work has documented overall decreasing linear trends of evaporation time series from Australia, New Zealand, China, former USSR and United States of America (Johnson and Sharma, 2010). However, we did not find reports for México. In addition, in those mentioned cases were not identified important frequencies. In our case study, linear regression analysis was used to estimate trends for 40 evaporation profiles; and power spectrum analysis was employed in order to identify important frequencies affecting evaporation anomaly time series behavior. We found negative linear trend for 27 out of 40 pan evaporation time series; and 18 of the 27 decreasing trends were significant at $p<0.05$. On the other hand, 13 pan evaporation trends were positive but only 3 at significant level ($p<0.05$). These

results suggest that negative trends are prevailing over positive trends when taking into account pan evaporation time series from Zacatecas state, México. These findings extend those of Linacre (2004), Gifford et al. (2005) and Johnson and Sharma (2010) who summarize overall negative trends for pan evaporation time series from Australia, New Zealand, China, former USSR and United States of America.

Our results provide compelling evidence that noise in these monthly pan evaporation series tends to be persistent (long-term memory, $D_s<1.5$) behavior, which suggest that long-term variation is more important than short-term variation in all analyzed profiles of pan evaporation. In addition, important frequencies noted in our study seem that could be related with the yearly cycle, quasi-biannual cycle, ENSO phenomena (2 to 7 years) and sunspots cycle (8 to 14 years). Most notably, these are important issues to take into account in future research to gain knowledge about the behavior of pan evaporation time series.

CONCLUSIONS

The overall mean of pan evaporation trends was -0.32 mm year^{-1}; whereas the mean of all significant trends was -0.53 mm year^{-1}. In addition, the mean of significant increasing evaporation trends was 1.09 mm year^{-1}, and the mean of significant decreasing evaporation trends was -0.79 mm year^{-1}. Noise in all 40 monthly pan evaporation series tends to be persistent (long-term memory, $D_s<1.5$) behavior, which suggest that long-term variation is more important than short-term variation. Important frequencies noted in most of the 40 evaporation anomaly time series seem to be related with the yearly cycle, quasi-biannual cycle, ENSO phenomena (2 to 7 years) and sun spots cycle (8 to 14 years).

ACKNOWLEDGEMENT

The authors are grateful for financial support by FoMix Zacatecas–CoNaCyT grant M0024–2005–1–16085.

REFERENCES

Brutsaert W (2006). Indications of increasing land surface evaporation during the second half of the 20th century. Geophys. Res. Lett., 33: L20403. doi:10.1029/2006GL027532.

Chattopadhyay N, Hulme M (1997). Evaporation and potential evapotranspiration in India under conditions of recent and future climate. Agric. For. Meteorol., 187: 55–73.

de la Fuente IM, Martínez L, Aguirregabiria JM, Veguillas J, Iriarte M (1999). Long–range correlations in the phase–shifts of numerical simulations of biochemical oscillations in experimental cardiac rhytms. J. Biol. Syst., 7: 113–130.

Evertsz CJG, Berkner K (1995). Large deviation and self–similarity analysis of curves: DAX stock prices. Chaos, Solitons and Fractals., 6: 121–130.

Gifford RM, Graham DF, Neville N, Michael LR (2005). Workshop summary on pan evaporation: An example of the detection and attribution of climate change variables. *In*: Gifford RM (editor). Pan Evaporation: An Example of the Detection and Attribution of Trends in Climate Variables.

Hausdorff JM, Peng CK (1996). Multiscaled randomness: A possible source of 1/f noise in biology. Phys. Rev., E 54: 2154–2157.

Huntington TG (2006). Evidence for intensification of the global water cycle: Review and synthesis. J. Hydrol., 319: 83–95.

Johnson F, Sharma A (2010). A Comparison of Australian Open Water Body Evaporation Trends for Current and Future Climates Estimated from Class A Evaporation Pans and General Circulation Models. J. Hydrometeorol., 11: 105–121.

Labitske K, Van Loon H (1989). Associations between the 11–year solar cycle, the QBO and the atmosphere. Part I: The troposphere and stratosphere in the northern hemisphere in winter. J. Atmosph. Solar–Terr. Phys., 50: 197–206.

Lawrimore JH, Peterson TC (2000). Pan evaporation trends in dry and humid regions of the United States. J. Hydrometeorol., 1: 543–546.

Linacre ET (2004). Evaporation trends. Theor. Appl. Climatol., 79: 11–21.

MacMynowski DG, Tziperman E (2008). Factors affecting ENSO's period. J. Atmosph. Sci., 65: 1570–1586.

Mandelbrot BB (1982). The Fractal Geometry of Nature. W.H. Freeman, New York.

Mendoza B, Lara A, Maravilla D, Jáuregui E (2001). Temperature variability in central México and its posible association to solar activiy. J. Atmosph. Solar–Terr. Phys., 63: 1891–1900.

Monetti RA, Havlin S, Bunde A (2003). Long–term persistence in sea–surface temperature fluctuations. Physica A., 320: 581–589.

Moreira JG, Kamphorst LDSJ, Oliffson KS (1994). On the fractal dimension of self–affine profiles, J. Phys. A. Math. Gen., 27: 8079–8089.

Mutziger AJ, Burt CM, Howes DJ, Allen RG (2005). Comparison of measured and FAO–56 modeled evaporation from bare soil, J. Irrig. Drain. Eng., 131(1): 59–72.

Peng CK, Buldyrev SV, Havlin S, Simons M, Stanley HE, Goldberger AL (1994). Mosaic organization of DNA nucleotides. Phys. Rev., E 49: 685–1689.

Quintana–Gomez RA (1998). Changes in evaporation patterns detected in northernmost South America. Proc. 7th Int. Meeting on Statistical Climatology. Whistler, BC, Canada, Institu. Mathematical Statistics., 97.

Roderick ML, Farquhar GD (2004). Changes in Australian pan evaporation from 1970 to 2002. Int. J. Climatol., 24: 1077–1090.

Secretaría del Medio Ambiente y Recursos Naturales (SEMARNAT) (2008). Volúmenes de recarga y extracción de acuíferos sobreexplotados. http://app1.semarnat.gob.mx/dgeia/cd_compendio08/compendio_2008/compendio2008/10.100.8.236_8080/archivos/03_Dimension_ambiental/01_Agua/D3_AGUA02_02.pdf. Downloaded 11th January, 2011.

Turcotte DL (1992). Fractals and Chaos in Geology and Geophysics. Cambridge University Press, Cambridge.

Valdez–Cepeda RD, Hernández–Ramírez D, Mendoza B, Valdés–Galicia J, Maravilla D (2003a). Fractality of monthly extreme minimum temperature. Fractals, 11: 137–144.

Valdez–Cepeda RD, Mendoza B, Díaz–Sandoval R, Valdés–Galicia J, López–Martínez JD, Martínez–Rubín de Celis E (2003b). Power–spectrum behavior of yearly mean grain yields. Fractals, 11(3): 295–301.

Weber RO, Talkner P (2001). Spectra and correlations of climate data from days to decades. J. Geophys. Res. D., 106: 20131–20144.

Wilks DS (1995). Statistical Methods in the Atmospheric science. Academic Press. ISBN 0–12–751965–3, p. 42.

Zubair L (2002). El Niño Southern Oscillation influences on rice production in Sri Lanka. Int. J. Climatol., 22: 249–260.